Biological Plausibility of Arm Postures Influences the Controllability of Robotic Arm Teleoperation

Sébastien Mick⬤, **Arnaud Badets**, Institut de Neurosciences Cognitives et Intégratives d'Aquitaine, Bordeaux, Nouvelle-Aquitaine, France, **Pierre-Yves Oudeyer**, Inria Bordeaux Sud-Ouest, Talence, France, **Daniel Cattaert**, Institut de Neurosciences Cognitives et Intégratives d'Aquitaine, Bordeaux, Nouvelle-Aquitaine, France, and **Aymar De Rugy**, Institut de Neurosciences Cognitives et Intégratives d'Aquitaine, Bordeaux, Nouvelle-Aquitaine, France, and University of Queensland, Brisbane, Australia

Objective: We investigated how participants controlling a humanoid robotic arm's 3D endpoint position by moving their own hand are influenced by the robot's postures. We hypothesized that control would be facilitated (impeded) by biologically plausible (implausible) postures of the robot.

Background: Kinematic redundancy, whereby different arm postures achieve the same goal, is such that a robotic arm or prosthesis could theoretically be controlled with less signals than constitutive joints. However, congruency between a robot's motion and our own is known to interfere with movement production. Hence, we expect the human-likeness of a robotic arm's postures during endpoint teleoperation to influence controllability.

Method: Twenty-two able-bodied participants performed a target-reaching task with a robotic arm whose endpoint's 3D position was controlled by moving their own hand. They completed a two-condition experiment corresponding to the robot displaying either biologically plausible or implausible postures.

Results: Upon initial practice in the experiment's first part, endpoint trajectories were faster and shorter when the robot displayed human-like postures. However, these effects did not persist in the second part, where performance with implausible postures appeared to have benefited from initial practice with plausible ones.

Conclusion: Humanoid robotic arm endpoint control is impaired by biologically implausible joint coordinations during initial familiarization but not afterwards, suggesting that the human-likeness of a robot's postures is more critical for control in this initial period.

Application: These findings provide insight for the design of robotic arm teleoperation and prosthesis control schemes, in order to favor better familiarization and control from their users.

Keywords: motor control, teleoperation, inverse kinematics, bio-inspired robotics, embodied cognition

INTRODUCTION

Given its number of joints, an anthropomorphic arm typically displays *kinematic redundancy* whereby there is an infinite number of arm postures that correspond to the same endpoint position in the 3D space (Baillieul & Martin, 1990). From a robotics-based perspective, inverse kinematic (IK) solving could be used to reduce the dimensionality of the control by relying on endpoint coordinates instead of joint angles as commands. Such dimensionality reduction could also be very valuable in the context of myoelectric prostheses, which use muscle activity as command signals to drive the artificial limb's motion. Indeed, compensating a higher level of amputation (e.g., humeral or shoulder level) requires more artificial degrees of freedom (DoF) to be controlled while having access to less command signals from residual muscles. However, IK solving requires a criterion with which to choose one posture among this infinity of available solutions. Regarding applications in robotic arm teleoperation or in prosthetics, the issue of which criterion to use is still open even though an intuitive option would consist in selecting human-like joint coordinations. Indeed, such a criterion would ensure consistency with the natural motion an anthropomorphic arm is meant to emulate, possibly favoring embodiment from the operator as well as controllability. However, to our knowledge, the influence of joint coordinations on the control of an artificial limb has yet to be explicitly addressed in the literature.

In this paper, we present an experiment where participants performed arm motion to drive a robotic arm placed next to them, so that its endpoint reached targets in a 3D workspace located in their field of view. To study the role of joint coordinations in this teleoperation setup, we designed two different IK solving criteria, selecting either biologically plausible or implausible postures to be displayed by the robot.

In this context, participants observed the robot as a humanoid agent moving in relation to their own motion, which may have elicited embodiment transfer toward the robot (Ogawa et al., 2012). Other related works (Imaizumi et al., 2016; Kalckert & Ehrsson, 2012; Longo et al., 2008) provide a definition of embodiment as a multifaceted phenomenon, its two major components being ownership (*Is this body mine?*) and agency (*Does this body move in accordance with my intentions?*). From a cognitive perspective, Imaizumi et al. (2016) describe ownership as "based on multisensory afferent inputs […] which are spatially and temporally congruent" and agency as related to the "congruence between a motor prediction based on an internal forward model […] and its predicted sensory feedback."

With regard to these definitions, we expected our experimental setup to address agency more than ownership, because the apparatus mostly stimulated the visual modality and provided no tactile feedback. In this context, when the robot displayed biologically plausible postures, the similarity between the robot's and participants' joint angles may have led the latter to feel like they effectively controlled these joints, thus reinforcing a sense of agency. Additionally, the location mismatch between the robot and a participant's actual body may have disturbed ownership without disrupting agency as much (Kalckert & Ehrsson, 2012). Regarding actual prosthesis use, Imaizumi et al. (2016) studied how embodiment toward a prosthetic arm affects its user's body posture and reported that agency plays a more decisive role than ownership in this mechanism. These works' findings support the rationale that biologically plausible joint coordinations would elicit embodiment transfer toward the robot more than biologically

implausible ones, possibly leading to better performance with the former than with the latter. Here, we specifically assessed this possibility during teleoperation of a robotic arm endpoint controlled in order to reach targets in 3D space.

Previous research in cognitive psychology provides relevant insight regarding how a participant is influenced by motion performed by an external agent. In particular, experiments by Kilner et al. (2003) and Press et al. (2005) investigated if a participant's own motion is disturbed when observing congruent or incongruent movements performed by another human or a robotic arm. While the former reported an effect when observing a human but not a robot's motion, the latter supported that visuomotor priming can be triggered by a robotic agent, and lead to interference with the participant's motion. Additionally, Bouquet et al. (2007) addressed how this priming relies on structural (e.g., shape, silhouette) or dynamic information (e.g., velocity, movement direction) conveyed by the moving agent. This study showed that the purely dynamic information conveyed by shapeless dots is enough to elicit interference when these dots exhibit biological motion. In the present study, we assessed how such interference might have an impact in a teleoperation context where the robotic arm is directly controlled by movements of the operator's arm.

In our experiment, both conditions of biological plausibility of postures convey identical structural information, given that the same robot is used throughout the experiment. However, the distinct joint coordinations associated with each condition convey different dynamic information, as they put the robot's joints in motion at different speeds and possibly opposite directions. Obviously, incongruency between performed and observed motion is more likely to happen when the robot displays biologically implausible postures. Therefore, we expect participants to perform better when the IK solving puts the robot in human-like postures. Our results confirmed that this was the case upon first exposure to our experimental conditions, but also revealed that the particular condition encountered first influences performance obtained with the other condition conducted afterward. In particular, performance

in the condition with biologically implausible postures was found to have benefited from initial exposure to the condition with biologically plausible ones.

METHODS

Participants

The study was conducted on a set of 22 able-bodied naive participants (13 male), aged 19–25 (mean 21.8; *SD* 1.13). All participants were right-handed and had normal or corrected to normal vision. None of them suffered from any mental or motor disorder that could affect their ability to perform the task. The experiment duration ranged from approximately 45 to 75 min, and no participant reported fatigue at the end of the experiment.

This study was carried out in accordance with the recommendations of the local ethics committee (CPP Île-de-France VII, Ref 2019-A01051-56). All participants gave written informed consent in accordance with the Declaration of Helsinki.

Apparatus

The participant was seated on a chair and asked to keep a straight back against the backrest. Twelve reflective spherical markers were attached to the participant's right arm with the help of armbands, so that each segment (upper arm, forearm and hand) had a set of four markers attached to it (Figure 1). In particular, the armband worn on the hand placed the participant's fingers so that the index was pointing forward and the other fingers were curled into the palm. Additionally, one of the four markers attached to the hand was fixed at the tip of a rod aligned with the index. This marker was referred to as the *driving marker* and represented the endpoint of the participant's arm. An optical motion tracking system (Optitrack V120 Trio & Motive software) was used to compute and record at 120 Hz the markers' positions and segments' orientations in the 3D workspace along time. A third-party software package (Astanin, 2016) allowed for real-time processing of the retrieved 3D data.

The controlled device was the robotic arm Reachy (Mick et al., 2019), designed to be employed as a tangible testbed for research on human-robot control strategies. This robot comprises seven DoF actuated by seven independent motors: three at shoulder level (flexion–extension, abduction–adduction, humeral rotation), two at forearm level (elbow flexion–extension, pronation–supination), and two at wrist level (radial–ulnar deviation, flexion–extension). Its end-effector is a single piece

Figure 1. Experimental setup: Both the robot and participant are facing the same way, in front of the targets. Credit © Gautier Dufau.

TABLE 1: 3D Coordinates of the Targets Relative to the Robot's Shoulder Center

Target	1	2	3	4	5
X—Rightward	0.04	0.2	0.13	−.03	−.12
Y—Forward	0.64	0.63	0.625	0.58	0.6
Z—Upward	0.06	−.1	−.3	−.4	−.15

Note. Values are in meter.

shaped like a human right hand in the same position as the participant's hand: index pointing forward, other fingers curled inside. Its size and proportions are similar to those of a human adult's arm, for a length of approximately 75 cm and a weight of about 1.4 kg.

The robot's shoulder was fixed on a wall-mounted support to the left of the participant. Additionally, a thirteenth marker was fixed at the tip of the robot's index and represented its endpoint. Both the robot and participant had their shoulder placed at a similar height and faced the same direction. A set of five virtual targets was located in the reachable space of the robot's endpoint. All targets were spheres of 25 mm in radius; the target centers' coordinates relative to the robot's shoulder center are reported in Table 1. Despite marking out a 3D zone, these targets were displayed using disks of foam padding as seen in Figure 1, in order to allow the robot's endpoint to physically enter the target zone. Each disk coincided with a target with respect to center coordinates and radius, and was placed vertically with the flat side facing the chair. In this way, participants were able to visually identify the targets' locations and size in the workspace. The foam disks were held in position with springs so that the assembly would not suffer major damage in case of shock with the robot, and would bring a disk back to its original location afterwards.

Custom software was developed in Python to carry out the experiment, record, and process data using several packages from the SciPy ecosystem (Virtanen et al., 2020).

Robot Control

In the framework of this experiment, participants drove the robot's endpoint by putting their own hand in motion in their peripersonal space. At any time, the 3D position of the driving marker was measured by the motion tracking system and used to compute the participant's endpoint's displacement vector relative to a reference position. This displacement vector was then scaled based on the participant's arm length and mapped to the robot's "peripersonal" space to determine the instantaneous 3D goal of the robot's endpoint. Commands were then sent to the robot's motors so that it would bring its endpoint on this goal.

Given that motors cannot instantly reach the angles sent as commands, a short delay remained between the robot's endpoint motion and the instantaneous goal's trajectory. This lag was found to usually dwell within the 350–450 ms interval during the control.

Posture Generation

In order to perform endpoint control on the robot, we used the IK solver IKPy (Manceron, 2015), which can compute a posture (i.e., a set of motor angles) that brings the robot's endpoint at a given 3D goal. Considering that the robot includes seven DoFs, its kinematic redundancy allows for an infinite number of solutions to this IK problem. We took advantage of this redundancy to design two posture generation strategies with similar endpoint accuracy but whose IK solving is biased toward two different ranges of postures. Drawing inspiration from a method described by Cruse (1986), we obtained such a bias by including a regularization term in the cost function underlying the IK solving. This term requires fourteen regularization parameters (two for each DoF); in this way, each strategy corresponds to a different set of parameters.

For each joint i, the first parameter is a regular angle α_i and the second is a weight w_i. As a result, for a given posture the total regularization term R, added in the cost function, is the

TABLE 2: Weights and Regular Angles Used to Bias IK Solving

Joint	ShFlex	ShAbd	HumMed	ElFlex	ForSup	UlnDev	WrExt
"Bio"							
Weight	0.013	0.013	0.0065	0.013	0.02275	0.026	0.026
Regular angle	0	20	0	75	0	0	0
"Non-bio"							
Weight	0.0075	0.015	0.0225	0.0075	0.025	0.0225	0.015
Regular angle	20	5	−25	70	40	25	35

Note. ShFlex = shoulder flexion; ShAbd = shoulder abduction; HumMed = Humeral lateral rotation; ElFlex = elbow flexion; ForSup = forearm supination; UlnDev = ulnar deviation; WrExt = wrist extension.

second-order norm of the weighted vector of the deviations to regular angles:

$$R = \sqrt{\sum_i \left(w_i \left(q_i - \alpha_i\right)\right)^2}$$

where q_i is the angular position of the joint i.

The set of regular angles defines an "ideal" posture toward which the solving will be biased; while the weights define the prominence of each joint in the total cost. A bigger weight on a given joint will result in a bigger impact of this joint's deviation to its regular angle on the regularization term. The weights and regular angles of each strategy are reported in Table 2.

The first posture generation strategy was designed to produce postures that would be biologically plausible relative to a human arm's reaching motion. To achieve this, regular angles were chosen to define this "ideal" posture so that it would be comfortable and appropriate as a resting stance for a human, with values far enough from joint boundaries (Figure 2(a) and (b)). Besides, the weight applied to humeral rotation was slightly lower than those of other joints, given the lighter effect of this joint's motion on the torques generated by gravity on the robot's actuators. Additionally, the three more distal joints of the robot (prono–supination, wrist flexion–extension, radial–ulnar deviation) were locked in a neutral position during the movements.

Conversely, the second strategy was designed to produce biologically implausible postures. With this aim, regular angles were chosen so that joints tend to be put outside of their comfortable range or near their angular boundaries.

In particular, postures generated with this strategy are biased towards bringing the elbow inside and displaying excessive supination, wrist extension and ulnar deviation (Figure 2(c) and (d)). The weights were also set in order to favor distal joint deviations over proximal ones when choosing the posture among IK solutions.

The first strategy was referred to as the "bio" strategy, whereas the second was labeled "non-bio" strategy. Please note that these labels are used out of convenience rather than to emphasize posture generation characteristics. In this way, the "bio" shorthand should stand for "bio-inspired" instead of "biomimetic" or "biological."

Task

The experiment relied on a target reach-and-hold task, where the participant was asked to drive the robot in order to bring its endpoint inside one of the five spherical targets and hold it in for 800 ms. At the beginning of the task, the participant's and robot's arms were placed in the same initial posture: humerus along the body, elbow flexed at 90°, vertical hand and index finger pointing forward. The beginning of the task was triggered by the experimenter and indicated to the participant by a short high-pitch beep sound. However, the task timer did not start until the participant's index moved further than 2 cm from its initial position. Then, the participant was given 15 s to complete the task.

During each task, custom software recorded the robot's joint angles measured by embedded sensors, as well as the participant's and robot's endpoint positions and arm links' orientations
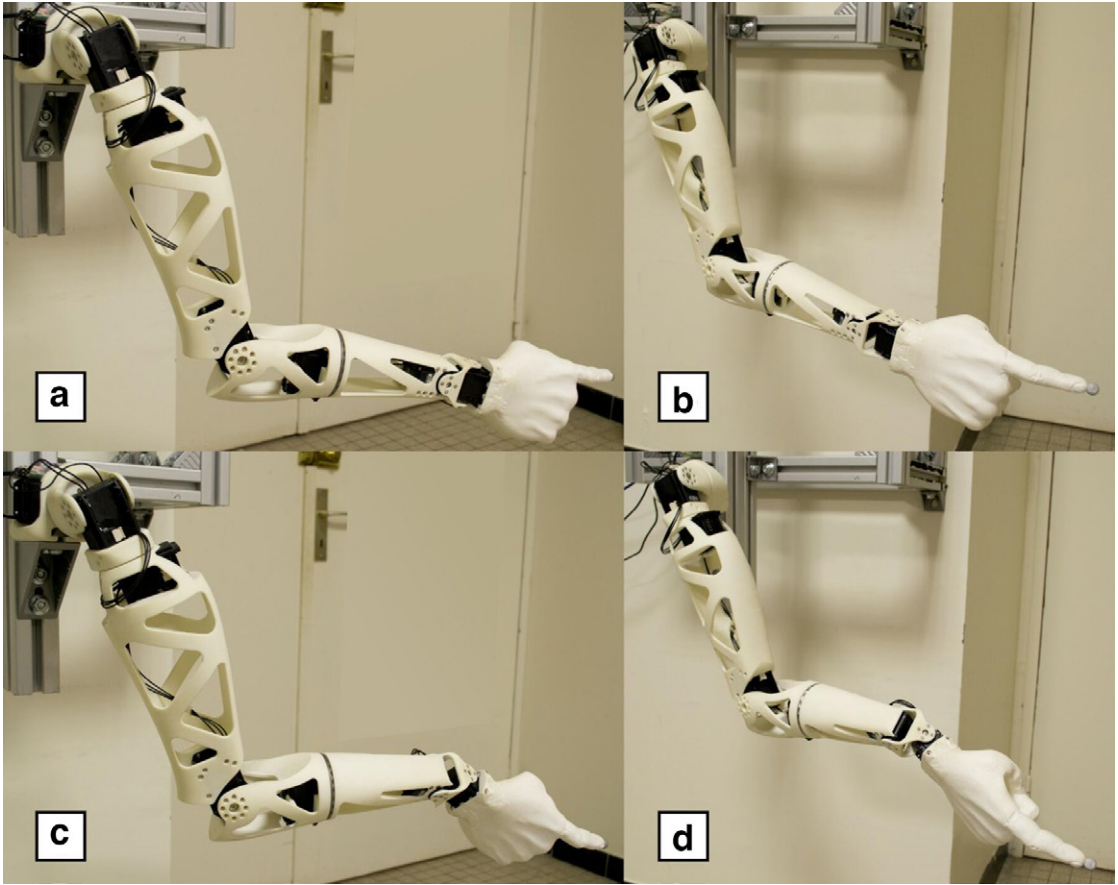
Figure 2. Average robot postures at the time of the first entry in the third target's zone. (a) and (b): with "bio" strategy. (c) and (d): with "non-bio" strategy.

measured by the motion tracking system. Whenever the robot's endpoint was located inside the target zone, an audio cue was played continuously, so that the participant was made aware that the endpoint was correctly placed. If it stayed continuously inside the target for 800 ms or if the 15 s time limit was reached, the task immediately ended and the outcome (success or failure) was recorded. At this point, the participant stopped having control over the robot, which was automatically brought back to the initial posture, and a low-pitch beep sound indicated the end of the task.

Protocol

Before the experiment started, the experimenter explained that during the control, the robot's endpoint was put in motion in accordance to the measured motion of the participant's hand. No further detail was provided to the participant regarding the posture generation or use of IK. After placing the recording devices, the experimenter introduced the task and described how the targets were virtual spheres displayed using disks of same radius. In this way, the participant was made aware of the goal, success conditions, and parameters of the experiment. Additionally, the experimenter demonstrated a "mock trial" by moving the robot manually while it was turned off, to introduce the task proceedings and corresponding audio cues. Participants did not perform any training or mock trial before the experiment started and had no previous experience with the robot's control system.
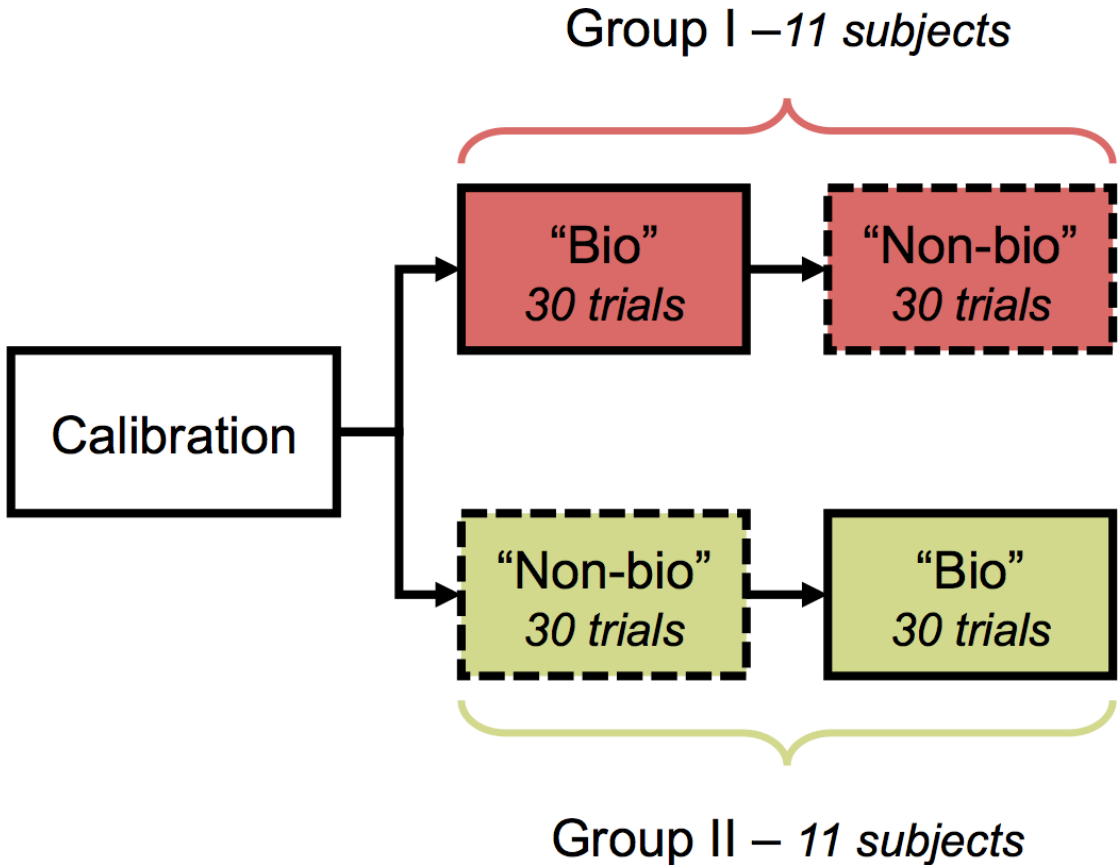
Figure 3. Experimental design: the pool of participants is divided in two groups of same size, each corresponding to a different order of experimental conditions.

An experimental phase repeated thirty trials of this task during which the posture generation strategy remained the same. Over a single phase, the target order was shuffled in a block-randomized fashion, so that two consecutive trials never corresponded to the same target. This order was common to all participants and phases. Each participant involved in the experiment performed two phases, one for each posture generation strategy, for a total of sixty trials. The phase order was shuffled so that half of the participants performed their first experimental phase using the "bio" strategy (Group I) while the other half began with the "non-bio" strategy (Group II). This experimental design is illustrated in Figure 3.

Data Analysis

At the end of the participant inclusion period, the recorded data were processed to allow for analysis. Due to measurement noise, the recordings from seventy-four trials (5.6% of the total dataset) were too heavily disrupted to allow for relevant data to be computed. Consequently, these trials were excluded from further analyses, while the rest of the trials formed the valid dataset.

Within the valid dataset, the success rate was found to be consistently excellent (>95%) over the population of participants, regardless of the posture generation strategy. This result confirms that the task was not too difficult for the participants but also highlights the need for other

criteria to evaluate how well they performed during the experiments.

In this way, we designed several quantitative metrics to assess the performance achieved during the task by addressing various dimensions of motor performance. These metrics were then used to compare the two posture generation strategies based on how well the participants controlled the robot.

- Approach Speed (AS)—This metric evaluates how fast the participants managed to drive the robot toward the target. For a given trial, provided the endpoint entered the target zone at least once, it is possible to determine the *approach time* that is, time elapsed since the starting zone's exit until the first entry in the target zone. Out of 1,246 valid trials, there was only one during which the target zone was never entered and for which no approach time could be determined. However, given that targets were placed at various distances from the starting zone, this time measurement is not appropriate as a target-independent metric. Instead, we used the *approach speed,* which is defined, for each target that was reached, as the ratio of the distance to the target by the approach time.
- Path Shortness (PS)—This metric addresses trajectory control and stability by evaluating the distance traveled by the robot's endpoint during a task, regardless of its duration. Indeed, an excessively long path can be associated with a poorer control of the robot, as it would be caused by wide deviations from the shortest path, or numerous goings and comings around the target. *Path shortness* is defined as the ratio of the total length of the endpoint's path by the length of the shortest path to the target.

To account for possible effects of phase order on the results, we conducted a four-class analysis by combining groups and experimental phase (Table 3). Each class includes data from eleven participants and is labeled according to the posture generation strategy (B and NB, respectively, standing for "bio" and "non-bio") and phase position (1 and 2, respectively, standing for first and second position).

We performed Kruskal–Wallis tests on the results from the two quantitative metrics to

TABLE 3: Four-Class Design Used to Carry Out Data Analysis

	"Bio" strategy	"Non-Bio" strategy
Group I	B1	NB2
Group II	B2	NB1

detect significant differences between classes. In all the cases where these tests indicated their existence, post hoc Mann–Whitney tests were performed to identify the pairs of classes presenting such differences. Bonferroni correction was applied accordingly, as multiple tests were carried out simultaneously. All relevant statistical values from these tests are reported in Table 4.

RESULTS

Participants' Arm Postures

The participants' joint angles were computed offline based on the recorded orientations of each link of the arm, while the robot's joint angles were recorded based on the measurements by the actuators' embedded sensors.

A qualitative analysis of the robot's joint angles confirmed that overall, the "bio" and "non-bio" strategies generated different postures for the robotic arm, as shown by the angle distributions at the time of the first entry in the target, illustrated in Figure 4. This difference is especially striking for the three more distal joints, as they were locked at a neutral zero angle in "bio" condition, and primarily encouraged for large deviation in "non-bio" condition.

Besides, this analysis revealed that the participants' joint angle distributions remained markedly similar over both experimental conditions. Median angles and amplitudes appeared to be quite close between "bio" and "non-bio" conditions for each of the seven joints.

Finally, this analysis allowed us to verify that the "bio" strategy generated postures similar to those of a human arm. Angle distributions between participants and robot in "bio" condition were found to be roughly similar for shoulder flexion and elbow flexion, while forearm supination, ulnar deviation, and wrist extension were centered on angles close to $0°$ for both

TABLE 4: Summary of Statistical Tests Performed on the Two Quantitative Metrics

| Metric | Kruskal–Wallis tests | | Mann–Whitney tests—Bonferroni Correction: 0.0083 | | | | | |
			B1 vs NB1	B1 vs B2	B1 vs NB2	NB1 vs B2	NB1 vs NB2	B2 vs NB2
Approach speed	$H = 41.619$	U	57,613	45,803	47,563	36,113	37,827	52,646
	$p = $ **4.8336e-9**	p	**1.1929e-6**	0.25967	0.94837	**4.8890e-9**	**1.9555e-6**	0.23560
Path shortness	$H = 42.471$	U	39,000	53,461	43,698	64,000	53,339	40,252
	$p = $ **3.1874e-9**	p	**2.8017e-4**	0.021966	0.091978	**1.6845e-10**	0.031764	**2.5091e-5**

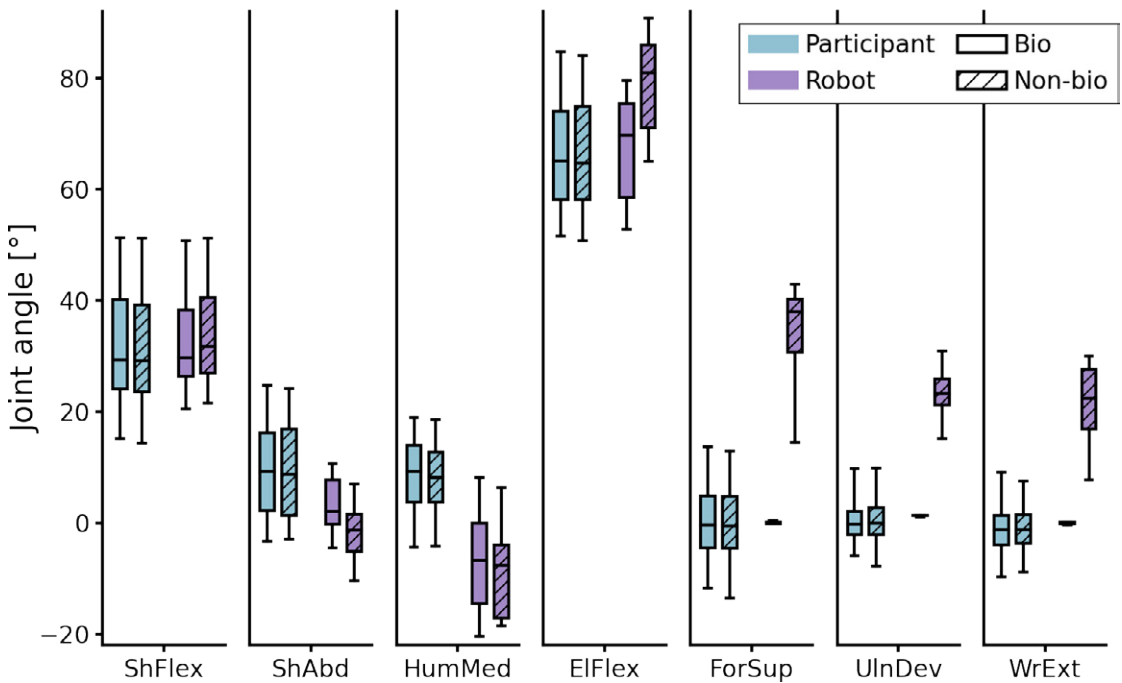*Note.* Significant differences are indicated by *p* values in bold.

Figure 4. Distributions of participants' and robot's joint angles at the time of the first entry in the target, with each posture generation strategy. Blue: participant; Purple: robot. Solid: "bio" condition; hatch pattern: "non bio" condition. ShFlex = shoulder flexion; ShAbd = shoulder abduction; HumMed = humeral lateral rotation; ElFlex = elbow flexion; ForSup = forearm supination; UlnDev = ulnar deviation; WrExt = wrist extension.

robot and participants. However, differences are noticeable for shoulder abduction and humeral rotation, indicating that some regularization parameters could be refined to produce more human-like postures.

Performance Metrics

Even though approach time was not considered a dependent variable, it was summarily analyzed to provide reference data. Its values ranged from 0.66 s to 12.92 s, with an average approach time of 2.87 s.

Regarding approach speed (Figure 5, left), the analysis revealed that approach periods were significantly slower when participants performed their first phase in "non-bio" condition. Indeed, the approach speed for class NB1 (median AS 7.47 cm/s) proved to be
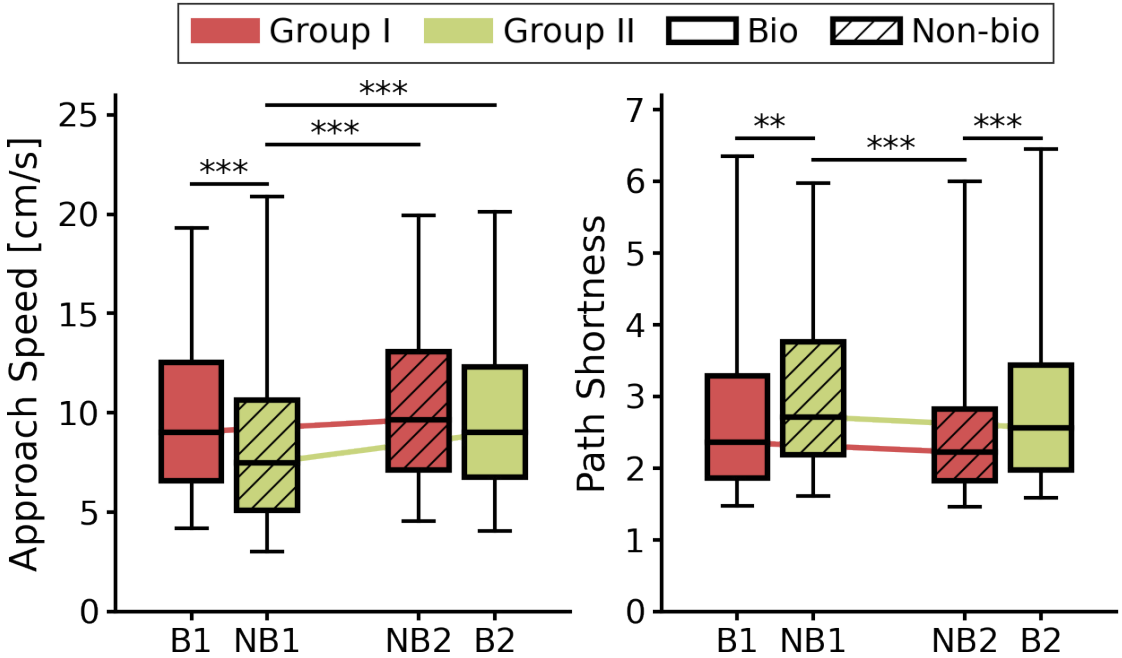
Figure 5. Boxplots of performance results based on *approach speed* (left) and *path shortness* (right). Red = Group I; gold = Group II. Solid = "bio" strategy; hatch pattern = "non-bio" condition. **$p < .001$; ***$p < .0001$.

significantly different from those of every other class (median AS >8.9 cm/s, $p < .0001$). In particular, when comparing classes B1 and NB1, that is, first phases of each group, this result suggests that the "bio" strategy makes it easier for participants to get accustomed to the robot's control. As such a difference is not found for second phases that is, between classes B2 and NB2, this may indicate that this effect decreases or even disappears after a period of initial exposure to the robot's control. We refer to this period as the *familiarization period*, which obviously takes place during the first experimental phase, but does not correspond to a distinct block of trials intended for participants to train on the task.

Regarding path shortness (Figure 5, right), significant differences were found between pairs B1 and NB1 ($p = 2.8017e-4$), NB1 and NB2 ($p = 1.6845e-10$), and NB2 and B2 ($p = 2.5091e-5$). In particular, endpoint paths were found to be significantly longer for class NB1 (median PS 2.71) than for class B1 (median PS 2.35), suggesting that the "non-bio" strategy elicits poorer robot control in the beginning of the experiment. Conversely, endpoint paths were shorter for class NB2 (median PS 2.22) than for class B2 (median PS 2.56). This may reveal that during their final phase, participants in Group I benefited from having used the "bio" strategy beforehand, whereas the performance of participants in Group II was impaired from having completed their first phase in "non-bio" condition.

DISCUSSION

Provided that posture similarity may increase the sense of agency (Imaizumi et al., 2016) and that incongruent movements were found to interfere with our own movement production (Bouquet et al., 2007; Press et al., 2005), we expected performance in robotic arm teleoperation to be affected by the biological plausibility of the postures used to operate it. Our results show that this is the case upon initial exposure

to the task, as participants performing their first phase in "bio" condition achieved better control (i.e., shorter paths and faster approach periods) than participants performing their first phase in "non-bio" condition. However, no similar effect was found when comparing performance in "bio" and "non-bio" conditions upon second exposure to the task, after a substantial familiarization has occurred in the initial phase conducted with the other condition. With regard to our hypothesis that a discrepancy between participants' and robot's postures would interfere with the control, this suggests that such an interference takes place more prominently during initial exposure to a novel control system, when familiarization occurs. This is consistent with findings reported by Dragan and Srinivasa (2014) showing that familiarization to a robotic arm motion can improve its predictability when natural movements are used, but that this mechanism saturates when using less natural movements. During the second phase of our experiment, participants may also have relaxed to the natural tendency we have to fixate the endpoint of an observed arm (Matarić & Pomplun, 1998), thereby not paying as much attention to the robot's postures as during the first phase where it was found to influence their performance. This appears consistent with several participants reporting that they did not notice a change in the robot's behavior between the two phases.

Additionally, when comparing performance obtained in the same condition but at a different phase of the experiment, our results indicate that the "non-bio" condition elicited better performance when employed in the second phase than in the first phase. Conversely, performance results were found to be similar between participants performing the "bio" strategy in the first or second phase. This suggests that participants performing the "non-bio" condition in the second phase have benefited from their previous experience with the "bio" strategy, whereas participants that performed the "bio" condition in the second phase did not benefit from, and may even have been hindered by, their previous experience with the "non-bio" condition. The condition in which the participants built their sensorimotor model of the robot's teleoperation

system may therefore be more critical than the joint coordinations used later on. Such interpretation of these findings accord with the guidance effect originally found in an observational paradigm (Badets & Blandin, 2004; Deakin & Proteau, 2000) where participants efficiently perform a motor skill when they have previously watched a relevant model of this skill. Accordingly, observing a model can improve the construct of a motor skill's cognitive representation that, in turn, efficiently guides subsequent physical practice.

It is worth noting that only two out of many possible posture generation strategies were assessed in this study. In particular, the corresponding two sets of regularization parameters were chosen for the satisfying tradeoff they offered between posture biasing, IK accuracy, and robot safety. Using the same IK solving method, other tradeoffs could be considered to achieve higher similarity or, conversely, higher dissimilarity with human postures when choosing regularization parameters. Additionally, such dissimilarity could be achieved through many different classes of postures, of which the one generated in our "non-bio" condition is merely an example. In this way, an alternative "non-bio" strategy biasing the solving toward a different class of biologically implausible postures could have led to more marked interference between robot and human motion, possibly accentuating the observed differences in performance.

It is also worth noting that although our fixation of the three most distal joints at 0° was well centered on the participants' actual arm movements for these joints (Figure 4), it is conceivable that this strict fixation has increased the predictability of the robotic arm behavior to a point that might have contributed to the observed pattern of results. This could be tested in the following work by maintaining high predictability despite non-biological postures, for instance by fixating these distal joints at implausible angles.

In practical terms, our results provide a basis for recommendations for the design of robotic arm teleoperation as well as upper-limb prostheses control systems. Although a prosthesis could obviously not be controlled with a valid

end-effector as in our current robotic arm tele-operation setting, the multiple artificial joints it contains could still benefit from a dimensionally reduced control strategy associated with partly automated kinematic control. In fact, to overcome the difficult issue of controlling more joints with less remaining muscles associated with high amputations, control schemes exploiting residual stump movements and kinematic regularities during natural reaching movements are being proposed (Kaliki et al., 2013; Merad et al., 2020). Following recent progresses in computer vision augmented with gaze information, contextual information about the goal of movement (e.g., the object to grasp) could also be determined automatically (González-Díaz et al., 2019; Pérez de San Roman et al., 2017), and might be used for robotic arm control in combination with IK solving (Mick et al., 2019). For those options or others, our results indicate that control schemes driving multiple joints at once should favor biologically plausible joint coordination, as this might facilitate controllability through congruency with motor intentions from a natural, valid arm's sensorimotor model, and possibly through embodiment via the sense of agency.

CONCLUSION

Humanoid robotic arm endpoint control is impaired (i.e., longer paths and slower approach periods) by biologically implausible joint coordinations experienced during the familiarization period but not afterwards. This suggests that the human-likeness of a robot's postures is more critical for the control in this initial familiarization period. These findings provide insight for the design of robotic arm teleoperation and prosthesis control schemes, in order to favor better familiarization and control from their users.

ACKNOWLEDGEMENTS

KEY POINTS

- Selecting biologically implausible postures to drive the robot was detrimental to its control by the participants while they are getting accustomed to the system's functioning.
- The human-likeness of robot postures is more critical in this familiarization period, as it affects later performance.
- It is preferable that arm prosthesis control schemes that involve multijoint control through IK solving favor biologically plausible joint coordinations.

FUNDING

ORCID iD

Sébastien Mick https://orcid.org/0000-0002-9900-6263

REFERENCES

Astanin, S. (2016). *A pure python library to receive motion capture data from Optitrack streaming engine.* https://pypi.org/project/optirx/.

Badets, A., & Blandin, Y. (2004). The role of knowledge of results frequency in learning through observation. *Journal of Motor Behavior*, *36*, 62–70. https://doi.org/10.3200/JMBR.36.1.62-70

Baillieul, J., & Martin, D. P. (1990). Resolution of kinematic redundancy. In *Proceedings of symposia in applied mathematics* (Vol. 41, pp. 49–89). American Mathematical Society.

Bouquet, C. A., Gaurier, V., Shipley, T., Toussaint, L., & Blandin, Y. (2007). Influence of the perception of biological or non-biological motion on movement execution. *Journal of Sports Sciences*, *25*, 519–530. https://doi.org/10.1080/02640410600946803

Cruse, H. (1986). Constraints for joint angle control of the human arm. *Biological Cybernetics*, *54*, 125–132. https://doi.org/10.1007/BF00320483

Deakin, J. M., & Proteau, L. (2000). The role of scheduling in learning through observation. *Journal of Motor Behavior*, *32*, 268–276. https://doi.org/10.1080/00222890009601377

Dragan, A., & Srinivasa, S. (2014). Familiarization to robot motion [Conference session]. In *Proceedings of the 2014 ACM/IEEE International Conference on Human-Robot interaction* (pp. 366–373). IEEE.

González-Díaz, I., Benois-Pineau, J., Domenger, J.-P., Cattaert, D., & de Rugy, A. (2019). Perceptually-guided deep neural networks for ego-action prediction: Object grasping. *Pattern Recognition*, *88*, 223–235. https://doi.org/10.1016/j.patcog.2018.11.013

Imaizumi, S., Asai, T., & Koyama, S. (2016). Embodied prosthetic arm stabilizes body posture, while unembodied one perturbs it. *Consciousness and Cognition*, *45*, 75–88. https://doi.org/10.1016/j.concog.2016.08.019

Kalckert, A., & Ehrsson, H. H. (2012). Moving a rubber hand that feels like your own: A dissociation of ownership and agency. *Frontiers in Human Neuroscience*, *6*, 40. https://doi.org/10.3389/fnhum.2012.00040

Kaliki, R. R., Davoodi, R., & Loeb, G. E. (2013). Evaluation of a noninvasive command scheme for upper-limb prostheses in a virtual reality reach and GRASP task. *IEEE Transactions on*

Biomedical Engineering, *60*, 792–802. https://doi.org/10.1109/TBME.2012.2185494

Kilner, J. M., Paulignan, Y., & Blakemore, S. J. (2003). An interference effect of observed biological movement on action. *Current Biology*, *13*, 522–525. https://doi.org/10.1016/S0960-9822(03)00165-9

Longo, M. R., Schüür, F., Kammers, M. P. M., Tsakiris, M., & Haggard, P. (2008). What is embodiment? A psychometric approach. *Cognition*, *107*, 978–998. https://doi.org/10.1016/j.cognition.2007.12.004

Manceron, P. (2015). *An inverse kinematics library aiming performance and modularity*. http://github.com/Phylliade/ikpy.

Mataríc, M. J., & Pomplun, M. (1998). Fixation behavior in observation and imitation of human movement. *Cognitive Brain Research*, *7*, 191–202. https://doi.org/10.1016/S0926-6410(98)00025-1

Merad, M., de Montalivet, E., Legrand, M., Mastinu, E., Ortiz-Catalan, M., Touillet, A., Martinet, N., Paysant, J., Roby-Brami, A., & Jarrasse, N. (2020). Assessment of an automatic prosthetic elbow control strategy using residual limb motion for transhumeral amputated individuals with socket or osseointegrated prostheses. *IEEE Transactions on Medical Robotics and Bionics*, *2*, 38–49. https://doi.org/10.1109/TMRB.2020.2970065

Mick, S., Lapeyre, M., Rouanet, P., Halgand, C., Benois-Pineau, J., Paclet, F., Cattaert, D., Oudeyer, P.-Y., & de Rugy, A. (2019). Reachy, a 3D-printed human-like robotic arm as a Testbed for Human-Robot control strategies. *Frontiers in neurorobotics*, *13*, 65. https://doi.org/10.3389/fnbot.2019.00065

Ogawa, K., Taura, K., Nishio, S., & Ishiguro, H. (2012). Effect of perspective change in body ownership transfer to teleoperated android robot. In *2012 IEEE RO-MAN: The 21st IEEE International Symposium on robot and human interactive communication* (pp. 1072–1077). IEEE.

Pérez de San Roman, P., Benois-Pineau, J., Domenger, J. -P., Paclet, F., Cataert, D., & de Rugy, A. (2017). Saliency driven object recognition in egocentric videos with deep CNN: Toward application in assistance to Neuroprostheses. *Computer Vision and Image Understanding*, *164*, 82–91. https://doi.org/10.1016/j.cviu.2017.03.001

Press, C., Bird, G., Flach, R., & Heyes, C. (2005). Robotic movement elicits automatic imitation. *Cognitive Brain Research*, *25*, 632–640. https://doi.org/10.1016/j.cogbrainres.2005.08.020

Virtanen, P., Gommers, R., Oliphant, T. E., Haberland, M., Reddy, T., Cournapeau, D., Burovski, E., Peterson, P., Weckesser, W., Bright, J., van der Walt, S. J., Brett, M., Wilson, J., Millman, K. J., Mayorov, N., Nelson, A. R. J., Jones, E., Kern, R., Larson, E., & SciPy 1.0 Contributors. (2020). SciPy 1.0: Fundamental algorithms for scientific computing in python. *Nature Methods*, *17*, 261–272. https://doi.org/10.1038/s41592-019-0686-2

Sébastien Mick received his MSc degree in engineering science from the Engineering School of Cognitics (Bordeaux Institute of Technology, France) in 2016, majoring in robotics. He is currently pursuing a PhD degree in cognitive science from Univ. Bordeaux (France) after joining the Aquitaine Institute for Cognitive and Integrative Neuroscience in 2017.

Arnaud Badets received a PhD degree in human movement sciences from Univ. Poitiers (France) in 2001. He is a CNRS researcher at the Aquitaine Institute for Cognitive and Integrative Neuroscience (Bordeaux, France), where he is leading a research team on the role of cognitive factors in motor control and learning.

Pierre-Yves Oudeyer received a PhD degree in artificial intelligence from Univ. Paris VI (France) in 2003. He is a research director at Inria and head of the Flowers Lab (Inria, Univ. Bordeaux & Ensta ParisTech). He studies lifelong autonomous learning and the self-organization of behavioral, cognitive, and language structures, at the crossroads of artificial intelligence, machine learning, and cognitive sciences.

Daniel Cattaert received a PhD degree in neuroscience from Univ. Bordeaux (France) in 1984. He is a CNRS researcher at the Aquitaine Institute for Cognitive and Integrative Neuroscience (Bordeaux, France). He specializes in the physiology of sensorimotor control in invertebrates, with interests in modeling neurons and neural networks.

Aymar de Rugy received a PhD degree in human movement sciences from University of the Mediterranean (Marseille, France) in 2001. He is a CNRS researcher at the Aquitaine Institute for Cognitive and Integrative Neuroscience (Bordeaux, France), where he is leading a research team on sensorimotor control in humans with applications in robotic and prosthesis control.